Energy Engineering

Tech Science Press

DOI: 10.32604/ee.2023.027968

ARTICLE

PSO-BP-Based Optimal Allocation Model for Complementary Generation Capacity of the Photovoltaic Power Station

Zhenfang Liu*, **Haibo Liu and Dongmei Zhang**

Department of Electrical Automation, Hebei University of Water Resources and Electric Engineering, Hebei University Water Conservancy Automation and Informatization Application Technology Research and Development Center, Cangzhou, 061001, China

*Corresponding Author: Zhenfang Liu. Email: zhanruo413933@163.com

Received: 24 November 2022 Accepted: 09 January 2023 Published: 01 May 2023

ABSTRACT

To improve the operation efficiency of the photovoltaic power station complementary power generation system, an optimal allocation model of the photovoltaic power station complementary power generation capacity based on PSO-BP is proposed. Particle Swarm Optimization and BP neural network are used to establish the forecasting model, the Markov chain model is used to correct the forecasting error of the model, and the weighted fitting method is used to forecast the annual load curve, to complete the optimal allocation of complementary generating capacity of photovoltaic power stations. The experimental results show that this method reduces the average loss of photovoltaic output prediction, improves the prediction accuracy and recall rate of photovoltaic output prediction, and ensures the effective operation of the power system.

KEYWORDS

Photovoltaic power station; complementary power generation; capacity optimization; resource allocation

1 Introduction

Photovoltaic power stations only generate electricity during the day, and their output is zero at night. In the daytime, due to the random change of weather conditions, the photovoltaic power will fluctuate greatly, and the power change can even reach 50% in a few minutes. To keep the grid frequency within the qualified range, when the output of photovoltaic power station increases, the conventional power supply in the grid needs to reduce its output, and the released load is supplied by photovoltaic power generation [1–2]. When the output of the photovoltaic power stations decreases, the output of the conventional power supply must increase rapidly to supplement the power shortage caused by the reduction of photovoltaic power generation. The natural characteristics of photovoltaic power generation determine the grid-connected operation of photovoltaic power plants, so it is necessary to optimize the configuration of the complementary power generation capacity of photovoltaic power plants and provide compensation and adjustment. Relevant scholars study the rational allocation of power generation capacity of photovoltaic power stations. Hou et al. [3] constructed the optimal allocation model of wind energy and solar energy storage capacity, which set up the evaluation index aiming at the total cost of the system, and obtained the wind-solar complementary characteristics, power loss rate, and contribution rate of the wind-solar hybrid power generation system. The Cat swarm algorithm is used to solve the model and optimize the indexes of the wind-solar-storage hybrid power generation system. However, this method has the problem of complicated calculation. Jin et al. [4] constructed the equivalent polymerization model of the large-scale photovoltaic power stations. By establishing a three-layer reactive power control strategy for photovoltaic power stations, the active and reactive power losses of the power grid can be obtained, the penetration rate of photovoltaics in the power grid can be improved, the voltage overflow problem of grid-connected large-scale photovoltaic power stations can be solved, and the stable operation of the power grid can be ensured. However, this method has the problem of data redundancy. Li et al. [5] built a photovoltaic energy storage complementary grid-connected power generation system model controlled by the virtual synchronous generator. Under the condition of load power fluctuation, it should take corresponding active power according to its capacity and adjust the power balance within the system. Establish an energy storage unit to release and store electric energy according to the fluctuation of photovoltaic output, and improve the tracking control effect of the maximum power point. However, this method has the problem of a long response time. Wang et al. [6] proposed a hybrid forecasting method for short-term photovoltaic power generation. The noise level is introduced, and the asymmetric photovoltaic power output function is established by using the complementary integrated empirical mode decomposition algorithm. According to the shape factor, crest factor, and kurtosis comprehensive factor, the IMF is adaptively divided into groups containing similar fluctuation components. Particle swarm optimization is used to optimize the parameters of the support vector machine, improve the global and local search ability, make particles traverse the global space, and enhance the local convergence performance. However, this method has a long time delay. According to the above research status, this paper considers natural conditions, regions, precipitation, and other factors, and adopts a particle swarm optimization algorithm to build the optimal allocation model of complementary power generation capacity of photovoltaic power stations, which solves the problems of complicated calculation, redundant data, and poor response effect. On this basis, a prediction model is established by using particle swarm optimization and BP neural network, which reduces the amount of data calculation. Markov chain model is used to correct the prediction error of the model, which reduces the calculation time and system delay. The weighted fitting method is used to predict the annual load curve, optimize the complementary power generation capacity, reduce the influence of rainy weather on the photovoltaic system forecast, and ensure the stable operation of the photovoltaic system.

2 Building PSO-BP Prediction Model

Particle Swarm Optimization has the characteristics of simple implementation, few adjustable parameters, and strong global search ability [7]. However, particle swarm optimization is easy to fall into the local optimal state. Combining with BP neural network can approximate any nonlinear continuous function with arbitrary precision, and can automatically extract the reasonable rules between output data and output data through learning in the training process [8]. At the same time, BP neural network can adaptively convert learning into weights, thus solving the problem of local optimal value. Therefore, the particle swarm optimization algorithm combined with BP neural network can effectively balance global exploration and local refinement, which is of great significance to grid-connected photovoltaic power generation and optimal resource allocation.

2.1 Design PSO-BP Algorithm Structure

BP neural network is a popular nonlinear mapping algorithm at present. The algorithm can be applied to the prediction of photovoltaic power generation output. Through the training and prediction of neural networks. Finally, the exact solution can be effectively approximated. However, this algorithm has the characteristics of backward propagation of errors and forward propagation of thresholds [9]. Its learning speed is slow, it is easy to fall into the local calculation and affect the overall progress, and its promotion ability is limited. It is not easy to predict PV system input curves [10–11].

Particle swarm optimization (PSO) can make up for the shortcomings of neural networks. The behavior of each particle of the algorithm is relatively simple and represents a possible solution [12]. Through population information, individuals and populations are continuously optimized to quickly find the optimal solution. The algorithm is simple to operate and easy to converge, so it can be widely used in function optimization and so on. Based on this, the parameter threshold and initial weight of the BP neural network are trained by the PSO algorithm. In this way, the prediction process of the PSO-BP algorithm is obtained as follows:

(1) According to the situation of the photovoltaic system, a neural network is constructed.
(2) Determines the number of particles in a particle swarm. And initialize the parameter threshold and initial weight of the BP neural network.
(3) After the two algorithms are combined, the advantages are complementary. Greatly improve the optimization speed of the whole algorithm.
(4) The PSO algorithm optimizes the most suitable two values above and returns them to the BP model for prediction.
(5) Use it for PV networks when the network meets performance requirements. Predict the outcome of its processing.

The specific PSO-BP algorithm prediction process is shown in Fig. 1.

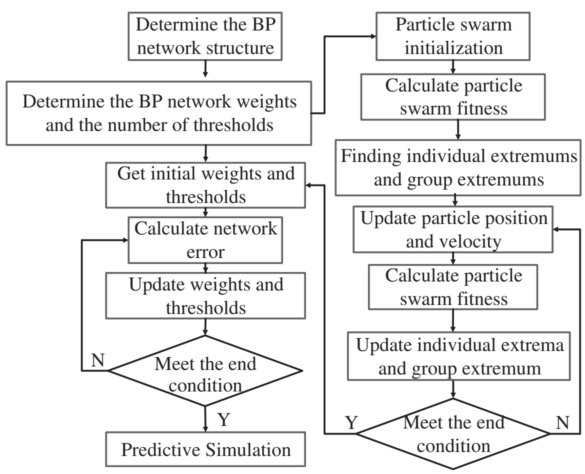

Figure 1: PSO-BP algorithm structure diagram

2.2 Correction of Structural Errors of PSO-BP Algorithm

To reduce the influence of natural environmental factors on the output of the photovoltaic systems. In this paper, the Markov chain model, which is widely used in time series models, is used to modify the structure of the PSO-BP algorithm. The Markov chain model has the "memoryless property", that is, the probability distribution of the next stage of the process depends only on the current state. Applicable scenarios are in line with different weather conditions in this paper.

Probability estimation for abnormal weather such as cloudy, rainy, hail, etc. Substitute the results into the original model to make the predicted results more accurate.

A Markov chain is composed of a series of discrete random variables, which are used in this paper to represent different weathers. Due to its memorylessness, the selection of its state is generally determined by conditional probability in the process. Its transition probability is defined as:

$$P_{ij}^{(k)} = P\left(X_{i+k} = S_j \,|X_i = S_i\right) \tag{1}$$

Among them, P_ij^((k)) represents the probability of state transition [13]. S stands for the state. X is a random parameter. k represents the number of steps.

For higher-order functions, the k-step transition probability of a Markov chain is expressed as:

$$P^{(k)} = \begin{bmatrix} P_{11}^{(k)} & P_{12}^{(k)} & \cdots & P_{1N}^{(k)} \\ P_{21}^{(k)} & P_{22}^{(k)} & \cdots & P_{2N}^{(k)} \\ \vdots & \vdots & & \vdots \\ P_{N1}^{(k)} & P_{N2}^{(k)} & \cdots & P_{NN}^{(k)} \end{bmatrix} \tag{2}$$

The relationship between the steps is represented by the correlation coefficient rk, and the weight of its influence is represented by uk, which is defined as:

$$r_k = \sum\nolimits_{i=1}^{N-k} \left[X\left(i\right) - \overline{X}\right]\left[X\left(i+k\right) - \overline{X}\right] \Big/ \sum\nolimits_{i=1}^{N} \left[X\left(i\right) - \overline{X}\right]^2 \tag{3}$$

$$u_k = |r_k| \Big/ \sum\nolimits_{k=1}^{K} |r_k| \tag{4}$$

The formula, $\overline{\mathrm{X}}$ represents the average value of random parameters [14]. K represents the step size of the Markov chain.

The probability distribution matrix P(t) for predicting the state of the PSO-BP model at time t is:

$$P\left(t\right) = \sum\nolimits_{k=1}^{K} u_k P\left(t-k\right)^k \tag{5}$$

2.3 Constructing Predictive PSO-BP Model

PSO-BP model aims at minimizing the output error of the BP neural network to learning samples, and optimizes the weights and thresholds of the BP neural network. A deep belief network is constructed by layer-by-layer superposition, and each CRBM in the network is trained layer by layer by the unsupervised greedy learning algorithm. Set the input amount as daily meteorological data, and determine the neuron state of the DBN network according to the change in photovoltaic power:

$$E_i = \varphi_i \sum_{i=1}^{n} \left(G_i P^{(k)} + z_i \xi\right) \tag{6}$$

where φ_i is the reconstructed value of the ith particle, n is the dimension of the particle, G_i is the output error of the network, z_i is the connection weight of the network, and ξ is the machine disturbance factor [15]. Choose a reasonable fitness function to calculate the fitness value of each particle:

$$t_i = \frac{\sum\limits_{i=1}^{n} E_i\left(s_p\right) - O_i \phi}{L_i} \tag{7}$$

where s_p is the capacity of the photovoltaic power station, O_i is the power generation, ϕ is the distance angle, and L_i is the active power [16]. When the change of the group extreme value meets the minimum limit or reaches the preset maximum iteration number, the global optimal solution is solved and the PSO-BP model is optimized:

$$D_i = \sum_{k-1}^{n} \psi_i(k) \times t_i \tag{8}$$

where ψ_i is the FM target power and k is the compensation integral coefficient.

2.4 Predicting PSO-BP Model Performance Indicators

There are many evaluation indicators for the prediction model of photovoltaic systems, to characterize the effect of photovoltaic output. This paper mainly uses two parameters of error percentage MAPE and root mean square error RMSE to describe the system performance. They are respectively defined as:

$$MAPE = \frac{1}{N}\sum\nolimits_{i=1}^{N}\left|\frac{P_{pi} - P_{mi}}{P_{mi}}\right| \times 100\% \tag{9}$$

$$RMSE = \frac{1}{P_N}\sqrt{\frac{1}{N}\sum\nolimits_{i=1}^{N}\left(P_{pi} - P_{mi}\right)^2} \tag{10}$$

In the above two expressions, P_{pi} represents the predicted power value of the photovoltaic power station at the ith time point. P_{mi} represents the real power value at that moment. N represents the total number of samples.

3 Optimal Configuration of the Photovoltaic System

Based on the complementary principle and characteristics of photovoltaic power plants, the PSO-BP forecasting model is solved by short-term optimal scheduling under the condition of determining the global optimal solution of multi-objective particle swarm optimization. In particle swarm iteration, the velocity of each particle swarm is:

$$v_i = \beta_i\lambda + c_1r_1(W_i + b_i) + c_2r_2(W_i + b_i) \tag{11}$$

where β_i is the individual extreme value of the i-th sample, λ is the inertia weight, c_1 and c_2 are learning factors, r_1 and r_2 are increasing the randomness of particle flight, W_i is the initial particle speed, and b_i is the random number of particle running speed. Based on obtaining the particle velocity, solve the particle position change:

$$v_\varphi = \frac{\theta_i W_n}{F\alpha} v_i \tag{12}$$

where θ_i is the influence of the i-th sample on the particle trajectory, W_n is the initial velocity of the particle, F is the best position experienced by the particle, and α is the random number of the position. The global optimal solution of the target particle swarm is obtained by formulas (8) and (9), and on this basis, the output power of the photovoltaic power station is calculated:

$$P_v = \left|\frac{L_v}{v_\varphi} - 1\right| K(v_i \times \varpi_L) \tag{13}$$

where L_v is the unit output power of photovoltaic power generation, $K(\cdot)$ is the Gaussian function, and ϖ_L is the marginal probability density function. After the photovoltaic power station is connected to photovoltaic power generation, the output during the day will be higher than that at night. Therefore, to ensure the base load output of the photovoltaic power station, it is necessary to establish power constraints:

$$H_j \geq H_{j\min} \tag{14}$$

where H_j is the output of the photovoltaic power station and $H_{j\min}$ is the minimum operating output of the photovoltaic power station. The photovoltaic power station needs to meet the heat capacity constraint on the branch to establish the power flow constraint, namely:

$$U_{j\min} \leq U_j \leq U_{j\max} \tag{15}$$

where $U_{j\min}$ is the upper limit of the node voltage U_j and $U_{j\max}$ is the lower limit of the node voltage U_j. Under the constraint conditions, the PSO-BP prediction model is solved:

$$R_i = \frac{\sum_{i=0}^{n} x_l D_i \left(\vartheta_i - y_j\right)}{C} \tag{16}$$

where x_l is the branch heat capacity, C is the number of neurons output, ϑ_i is the light intensity, and y_j is the expected value of the j-th output of the samples. According to the output weights of neurons, the expected output values in the new data set of training samples are defined, to complete the expected output of the single implicit feed forward neural network and realize the solution of the algorithm model.

4 Experimental Results and Analysis

4.1 Experimental Dataset

Before the experiment, images of 7 kinds of target equipment such as cabinets and servers of photovoltaic power plants were obtained, and a data set was established. And establish the basis for intelligent image recognition through image preprocessing. The selected photovoltaic power station will be connected to the grid on July 19, 2021. A dual-axis tracking photovoltaic array was established by using a crystalline silicon module and Huawei 50 kW series inverter. When considering the training of the PSO-BP model, it is necessary to keep the image size consistent. Therefore, it is unified into 224224 and 299299 in this paper.

Aiming at the characteristics of deep convolutional neural networks that require a high number of training samples. In this paper, the method of data augmentation is used to train the model. The specific training methods are as follows: (1) In the plane where the image is located, move the image for a certain distance in a certain direction. (2) Enlarge or reduce the image, and restore the changed image to its original size by cropping or filling. (3) Change the image orientation by rotation. (4) Set the interference conditions. (5) Adjust the image brightness and contrast to change its visual effect.

4.2 The Overall Process of the Experiment

The entire testing process is divided into three parts:

(1) Set up the computer vision development environment and get the best weights for the YOLO test model through training and testing. According to the standard of obvious features and comprehensive classification, 8851 pictures were screened, and the experimental data set was determined.

(2) According to the variety of image content, the data is preliminarily divided into seven categories as shown in Table 1. Images of the above categories were classified using the image annotation software labeling. And according to the ratio of 5:1:1 to allocate image sample sets, as shown in Table 1.

Table 1: Data set sample distribution

Numbering	Equipment category	Training samples	Validation samples	Test sample	Total
01	Cabinet	553	100	100	753
02	Server	836	200	200	1236
03	Monitor	859	150	150	1159
04	UPS	593	100	100	793
05	Switch	869	200	200	1269
06	Router	1193	200	200	1593
07	Other devices	1448	300	300	2048

(3) According to the sample distribution of the dataset shown in Table 1. The YOLO test model is used for detection and identification, as shown in Fig. 2.

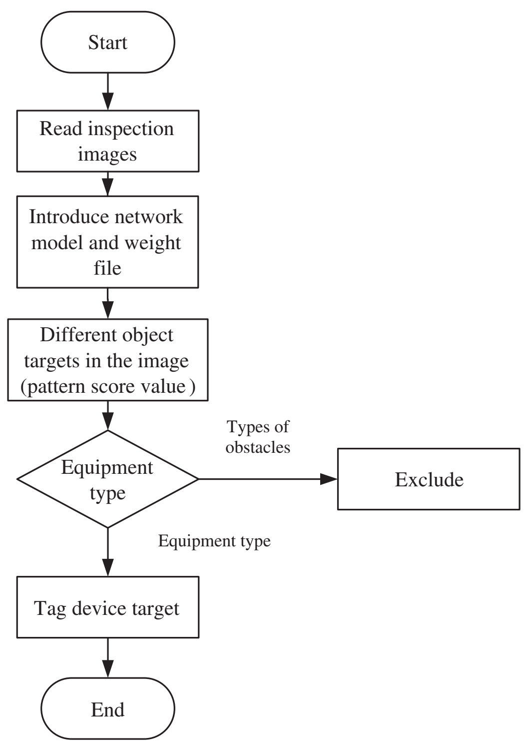

Figure 2: Target detection identification flow chart

(4) In the above experimental environment settings, the proposed algorithm is compared with the methods of reference [3], methods of reference [4], methods of reference [5], and methods of reference [6]. And record the detection and evaluation results of each algorithm.

4.3 Analysis of Results

4.3.1 Average Loss Analysis

The average loss data set is divided into three parts: training set, verification set, and test set. When training the model, the validity of the model is often diagnosed according to the average loss of the training set and the average loss of the verification set. The average loss curve is used to verify the accuracy of the neural network. The better the curve fitting effect, the better the training effect of the method to optimize parameters. The average loss curve results of five different methods are shown in Fig. 3.

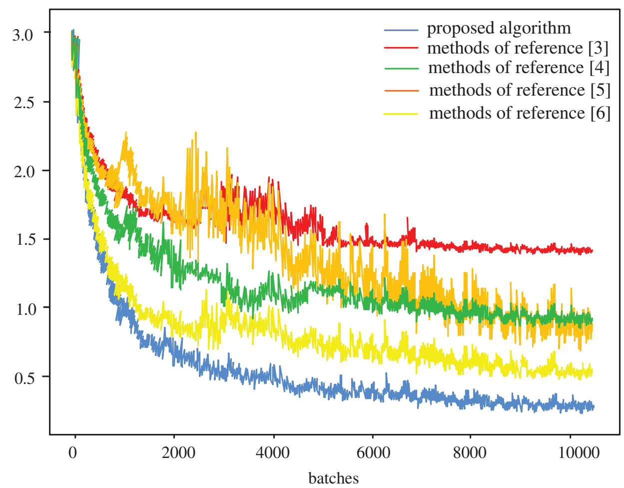

Figure 3: Average loss curve

According to Fig. 3, the loss value of the proposed method decreases greatly at the beginning of training, indicating that the learning rate is suitable for gradient decline. After learning to a certain stage, the loss curve tends to be stable, and the minimum value is about 0.3. However, the loss values of the methods in reference [3] and reference [5] fluctuate greatly, and the methods in reference [4] and reference [6] gradually converge after a long repetition. It shows that the proposed method has good stability. This is because the proposed method adopts BP neural network, which adaptively converts learning into weights in the training process.

4.3.2 Accuracy of Analysis

Accuracy is the most intuitive evaluation index of machine learning. In the case of balanced positive and negative samples, the accuracy of equipment identification of different methods is tested. The closer the accuracy rate is to 100%, the higher the effectiveness of the method. The test results are shown in Table 2.

Table 2: Comparison of recognition accuracy of different models

Equipment category	The recognition accuracy of each model/%				
	Proposed algorithm	Methods of reference [3]	Methods of reference [4]	Methods of reference [5]	Methods of reference [6]
01	98.77	95.74	96.37	96.18	95.74
02	97.52	96.12	94.20	95.31	95.39
03	96.84	94.38	95.91	94.28	94.64
04	98.82	95.57	96.73	95.84	95.47
05	97.49	96.59	95.19	94.72	96.18
06	98.13	95.69	95.34	94.18	95.30
07	96.88	94.74	95.17	96.07	94.84

According to Table 2, the accuracy rate of the proposed method is high, and the average accuracy rate can reach 97.78%. However, the average accuracy of reference [3] is 95.55%, that of reference [4] is 95.56%, that of reference [5] is 95.23%, and that of reference [6] is 95.37%. The main reason is that the model in this paper uses the Markov chain model to correct the model prediction error and improve the model recognition ability.

4.3.3 Recall Rate of Analysis

The recall rate is a measure of coverage, and many positive examples of the measure are divided into positive examples. As far as image samples are concerned, the recall rate results can verify how many positive examples in the samples are predicted correctly. The higher the recall rate, the more retrieved content, and the better the effect of the method. The recall rates of five different methods are tested, and the test results are shown in Table 3.

Table 3: Comparison of identification recall rates of different models

Equipment category	The recognition rate of each model/%				
	Proposed algorithm	Methods of reference [3]	Methods of reference [4]	Methods of reference [5]	Methods of reference [6]
01	97.45	96.98	94.28	95.94	94.71
02	96.17	95.46	95.78	95.43	94.04
03	98.28	96.84	96.64	96.14	96.55
04	97.35	95.96	94.94	94.87	96.04
05	96.38	94.39	95.75	95.34	95.32
06	96.17	95.74	94.04	95.18	94.94
07	97.47	94.48	95.51	96.42	96.73

According to Table 3, the recall rate of the proposed method is high, and the average recall rate can reach 97.04%. The average recall rate of reference [3] is 95.69%, that of reference [4] is 95.28%, that of reference [5] is 95.62%, and that of reference [6] is 95.48%. The main reason is that this model uses a particle swarm optimization algorithm to identify samples in a fast global search way, thus improving the detection coverage effect of the target to be detected.

5 Conclusion

To optimize the complementary power generation capacity of the photovoltaic power stations and improve the precision of photovoltaic power station equipment. In this paper, considering the influence of different external factors, the PSO-BP algorithm structure is used to establish a photovoltaic power station prediction model to realize multi-target detection. The experimental results show that the average loss of this method is low, and the curve-fitting effect is excellent. After a certain stage of learning in the training process, the loss curve tends to be stable, and the minimum value is about 0.3. When the positive and negative samples are balanced, the accuracy of this method is high, reaching 97.78%. The more searched content, the higher the recall rate of this method, and the average recall rate can reach 97.04%. Therefore, the proposed method can provide a data basis for the configuration of complementary power generation capacity of photovoltaic power plants, and provide theoretical support for the subsequent intelligent identification of equipment and the design of the control system.

Funding Statement: The authors received no specific funding for this study.

Availability of Data and Materials: The data used to support the findings of this study are available from the corresponding author upon request.

Conflicts of Interest: The authors declare that they have no conflicts of interest to report regarding the present study.

References

1. Yang, D., Wang, S. W., Wang, Y., Chen, B., Zheng, T. R. et al. (2019). Optimal complementary photovoltaic capacity configuration for grid-connected wind farms expansion. *Journal of Shandong University (Engineering Science), 49(5),* 44–51.
2. Fu, H. B., Xu, J., Liao, S. Y., Li, X., Jiang, Z. (2019). Source-load tracking technology of distribution network based on model predictive control. *Southern Power System Technology, 13(4),* 93–99.
3. Hou, H., Xu, T., Wu, X., Wang, H., Chen, Y. (2020). Optimal capacity configuration of the wind-photovoltaic-storage hybrid power system based on gravity energy storage system. *Applied Energy, 271,* 115052. https://doi.org/10.1016/j.apenergy.2020.115052
4. Jin, L. J., Gong, X. J., Sun, Q. Y., Sha, M. C. (2021). Reactive powercontrol of grid-connected photovoltaic power generation. *Journal of Physics: Conference Series, 1754(1),* 1–6. https://doi.org/10.1088/1742-6596/1754/1/012001
5. Li, C., Yuan, S. (2020). Research on frequency modulation control of photovoltaic power generation system based on VSG. *International Journal of Low-Carbon Technologies, 16(2),* 287–293. https://doi.org/10.1093/ijlct/ctaa054
6. Wang, L., Liu, Y., Li, T., Xie, X. Z., Chang, C. M. (2020). The short-term forecasting of asymmetry photovoltaic power based on the feature extraction of PV power and SVM algorithm. *Symmetry, 12(1),* 1–20. https://doi.org/10.3390/sym12111777
7. Priyadarshi, N., Padmanaban, S., Holmnielsen, J. B., Bhaskar, M. S., Azam, F. (2021). Internet of things augmented a novel PSO-employed modified zeta converter-based photovoltaic maximum power tracking system: Hardware realisation. *IET Power Electronics, 13(13),* 2775–2781. https://doi.org/10.1049/iet-pel.2019.1121

8. Hu, K., Wang, L., Li, W., Cao, S. H., Shen, Y. Y. (2022). Forecasting of solar radiation in photovoltaic power station based on ground-based cloud images and BP neural network. *IET Generation, Transmission & Distribution, 16(2),* 333–350. https://doi.org/10.1049/gtd2.12309
9. Jiang, F., Wang, Z. Y., Zhang, P. (2019). Forecasting power generation of solar photovoltaic system based on the combination of grey model and weighted Markov chain. *Power System Protection and Control, 47(15),* 55–60.
10. Liu, L. Q. (2020). Image recognition algorithms based on deep convolution generative adversarial network. *Chinese Journal of Liquid Crystals and Displays, 35(4),* 383–388. https://doi.org/10.3788/YJYXS20203504.0383
11. Zhang, W. Z., Hu, Z. K., Li, X. L. (2020). Convolutional neural image recognition algorithm based on LeNet-5. *Chinese Journal of Liquid Crystals and Displays, (5),* 486–490. https://doi.org/10.3788/YJYXS20203505.0486
12. Yin, Y. Q., Gong, H. J., Wang, X. H. (2020). Embedded real-time video object detection algorithm based on YOLOv3. *Computer Engineering, 46(2),* 230–234.
13. Wang, W., Zou, T., Wang, X. (2020). Image classification method based on D-MobileNet model. *Application Research of Computers, 37(4),* 1261–1264 +1270.
14. Yang, W., Zhou, K. X., Liu, J. J., Zhang, Z. W., Wang, T. (2019). Method of dry and wet state recognition of pavement based on migration learning and Inception-v3 model. *China Sciencepaper, 14(8),* 912–916.
15. Zhang, X. D., Gu, Z. Q., Qin, X. F. (2019). VGG16 model-based fast loop closure detection algorithm. *Optical Instruments, 41(3),* 20–26.
16. Chen, Y. Y., Gong, C. Y., Liu, Y. Q., Fang, X. M. (2019). Fish identification method based on FTVGG16 convolutional neural network. *Transactions of the Chinese Society for Agricultural Machinery, 50(5),* 230–238.